14th Australasian Fluid Mechanics Conference
Adelaide University, Adelaide, Australia
10-14 December 2001

A Numerical Study of Swirling Vortex Rings

A. Ooi[1], J. Soria[2], T. T. Lim[3], W. Kollmann[4] and M. S. Chong[1]

[1]Department of Mechanical and Manufacturing Engineering
University of Melbourne, Victoria, 3010 AUSTRALIA

[2]Department of Mechanical Engineering
Monash University, P.O. 31, Victoria, 3800 AUSTRALIA

[3]Department of Mechanical Engineering
[3]National University of Singapore, 10 Kent Ridge Crescent, 119260 SINGAPORE

[4] Department of Mechanical Engineering
University of Califarnia, Davis, CA 95616 USA

Abstract

The evolution of the axisymmetric swirling vortex ring is studied by solving the Navier-Stokes equations in cylindrical coordinates. Simulations were carried out at various Reynolds numbers, *Re*, and swirl numbers, *S*. It was found that the propagation velocity of the vortex ring decreases with increasing *S*. It is shown that this is due to the presence of secondary vorticity at the front of the ring which is of the opposite sign to the primary vortex ring.

Introduction

The term "vortex ring with swirl" refers to a vortex ring with an azimuthal component of velocity. From the fundamental viewpoint, the swirling vortex ring is an interesting flow case where a careful study may be conducted on the detailed mechanism of vortex stretching. In the absence of swirl, all vortex lines are circular and stretching is proportional to the change in circumference of a circular vortex line as it approaches or moves away from the axis of symmetry. However, for a swirling vortex ring, coupling of swirl and meridional flow also causes reorientation of the vortex lines, hence additional stretching ([10]). From a more practical point of view, the study of vortex rings with swirl may provide vital information to enhance our understanding of an axisymmetric or "bubble" type vortex breakdown which is known to occur in the leading edge vortices of a highly swept wing at high angle of attack (see [8] and [10]).

The study of the vortex rings with swirl has so far been limited to theoretical analyses with most work concentrating mainly on obtaining steady solutions of the Euler equations (see [2], [5] and [9]). Recently, [10] carried out a numerical study of the dynamics of initially polarized isolated viscous vortex rings (which include vortex rings with swirl) through vorticity transport equations using divergence free axisymmetric eigenfunctions of the curl operator. Their results are consistent with the force-balance argument (see [7], [12] and [6]) which show that if the vortex core is thin, the propagation velocity of the vortex ring decreases with increasing swirl. However, [10] further shows that even if the cores are thick, vortex rings still exhibit the same behaviour, even for Hill's spherical vortex with weak swirl.

Apart from the theoretical and numerical works, limited experiments on a vortex ring with swirl has been carried out by [4]. The results obtained were not conclusive due to the contamination by spurious vorticity entering the vortex ring during generation. The difficulties faced by [4] in obtaining conclusive results leads us to the present numerical study with the aim of getting a better understanding of how the azimuthal component of velocity (i.e. the swirl) affects the behaviour and the topological structure of viscous vortex rings. One of the advantages of the numerical simulation over the experiment is that we can easily control the initial flow parameters.

Numerical Model

The axisymmetric Navier-Stokes equations in cylindrical coordinates are given by

$$\frac{\partial v_r}{\partial t} = -v_r\frac{\partial v_r}{\partial r} - v_z\frac{\partial v_r}{\partial z} + \frac{v_\theta^2}{r} - \frac{1}{\rho}\frac{\partial p}{\partial r} + \frac{1}{Re}\left[\frac{\partial}{\partial r}\left(\frac{1}{r}\frac{\partial}{\partial r}(rv_r)\right) + \frac{\partial^2 v_r}{\partial z^2}\right] \quad (1)$$

$$\frac{\partial v_\theta}{\partial t} = -v_r\frac{\partial v_\theta}{\partial r} - v_z\frac{\partial v_\theta}{\partial z} - \frac{v_\theta v_r}{r} + \frac{1}{Re}\left[\frac{\partial}{\partial r}\left(\frac{1}{r}\frac{\partial}{\partial r}(rv_\theta)\right) + \frac{\partial^2 v_\theta}{\partial z^2}\right] \quad (2)$$

$$\frac{\partial v_z}{\partial t} = -v_r\frac{\partial v_z}{\partial r} - v_z\frac{\partial v_z}{\partial z} - \frac{1}{\rho}\frac{\partial p}{\partial z} + \frac{1}{Re}\left[\frac{1}{r}\frac{\partial}{\partial r}\left(r\frac{\partial v_z}{\partial r}\right) + \frac{\partial^2 v_z}{\partial z^2}\right] \quad (3)$$

where v_r, v_θ and v_z are the radial, azimuthal and axial components of velocity. For an ordinary vortex ring (without swirl), $v_\theta = 0$ everywhere and the only non-zero component of vorticity is ω_θ. In general, for a swirling vortex ring, all three components of velocity and vorticity are non-zero.

The axisymmetric Navier-Stokes equations is solved using a hybrid Fourier-finite difference method. A fifth order upwind biased scheme is used for the convective terms and a fourth order central finite difference scheme is used for the viscous terms. In all simulations described in this paper, 95 and 251 grid points were used in the radial and axial directions respectively. Coordinate mapping is used in both directions to ensure that most of

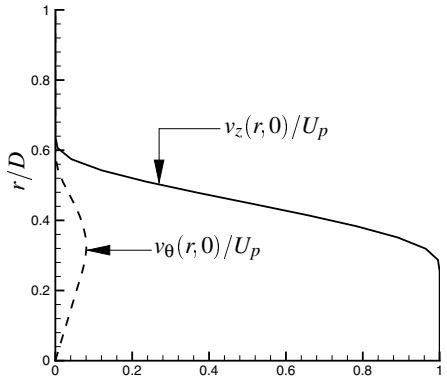

Figure 1: Inlet profiles for v_z and v_θ for $S = 0.1$.

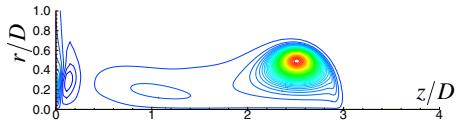

Figure 2: Contours of ω_θ for Re=1727 and S=0.0.

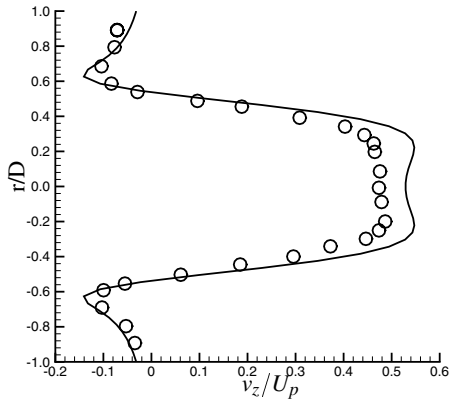

Figure 3: Comparison of v_z at $z/D = 2.5$ with experimental data of [11]. ——— current computation, ◦ experimental data of [11].

the grid points are clustered close to the inlet and axis of symmetry (see [3] for more details on the numerical method).

The Reynolds number, Re, is defined as

$$Re = \frac{U_p D}{\nu}, \tag{4}$$

where U_p is the maximum piston velocity and D is the piston diameter. The swirl component is introduced according to the swirl number, S, defined by [1] to be

$$S = \frac{2v_\theta(r/2,0)}{v_z(r/2,0)}. \tag{5}$$

The velocity profile used at the inlet for $S = 0.1$ is shown in figure 1.

In this paper, we will attempt to simulate the vortex ring generated by the motion according to [11]. The piston motion consists of a linear acceleration followed by constant speed motion and linear deceleration to zero velocity. The piston motion is modelled in the simulation by prescribing velocity profiles for v_z and v_θ (shown in figure 1) at the inlet with amplitude following the experimental piston motion.

It must be noted that the method for generating the initial swirling vortex ring in this paper is different to the method used in [10]. There, a swirling vortex ring (obtained from a linear combination of the left- and right-handed components of a Helical Wave Decomposition) is specified as an initial condition in the computations. In this study, the initial condition is a quiescent fluid. The swirling vortex ring is generated by ramping up the inlet profile (shown in figure 1), keeping it at constant amplitude for a short period of time, followed by a linear deceleration. This is a numerical approximation of an experimental situation where the axial and rotational motion of a piston is used to create swirling vortex rings with different values of S.

Results and Discussion

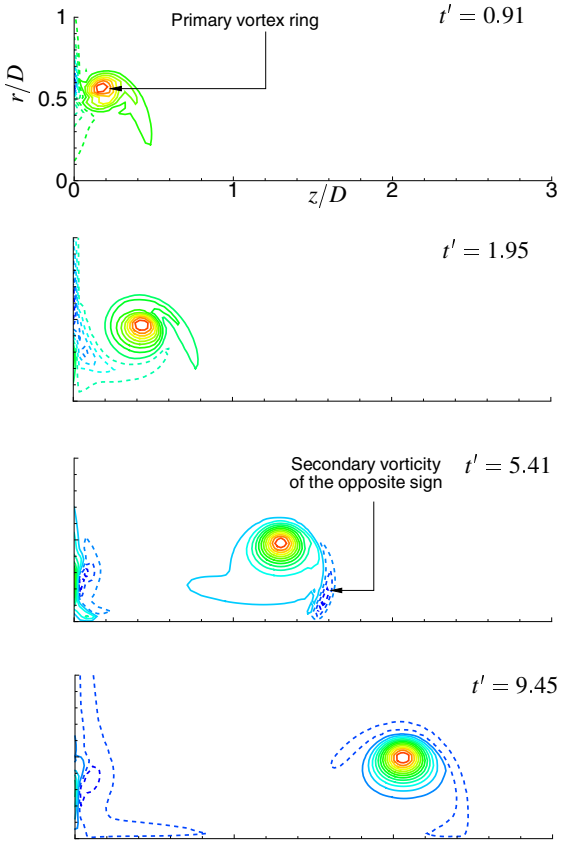

Figure 4: Evolution of contours of ω_θ for Re=4020 and S=0.1. $t' = tU_p/D$

As a reference, a simulation was carried out at $Re = 1727$ with $S = 0$. Contours of ω_θ when the vortex ring is at $z/D = 2.5$ are shown in figure 2. The ring shows the typical head-tail structure reported in [10]. Since experimental data for this case is available (see [11]), a more quantitative test of the accuracy of the numerical method is possible. Figure 3 shows the radial distribution of axial velocity, v_z, at $z/D = 2.5$. Results from the

current simulation compares well with experimental data. The slight differences in the experimental and numerical data can be explained by what is happening at the pipe outlet. In the experiment, the velocity profile is not exactly the top hat profile as was used in the simulations. Furthermore, in the experiment, the pipe extends into the flow field. The consequence of the numerical model for the entrance condition is that the start up vortex, which moves into the pipe in the experiments, has no place to go in the simulations and remains near the entrance section and interacts with the wall boundary (see left side of figure 2). It must be mentioned here that the presence of the start up vortex have no influence on the results below as we have managed to qualitatively reproduce the numerical data in [10] which was obtained without the presence of the "numerical" pipe.

Numerical simulations of swirling vortex rings were carried out at $Re = 1727$ and $Re = 4020$ with $S = 0.1$, 0.2 and 0.5. Evolution of the contours of ω_θ for the simulation at $Re = 4020$ with $S = 0.1$ is shown in figure 4. Initially, a primary vortex ring is formed due to the shear layer at the inlet. This primary vortex ring is convected downstream. At later times, a weaker secondary ring of the opposite sign (shown as dashed contour lines) is formed close to the axis of symmetry. Due to the presence of the primary vortex ring, this patch of secondary azimuthal vorticity is convected away from the axis of symmetry in the radial direction, eventually moving in front of the primary vortex ring. The primary vortex ring actually moves faster than the secondary vorticity and will eventually drag the secondary vortex ring over it.

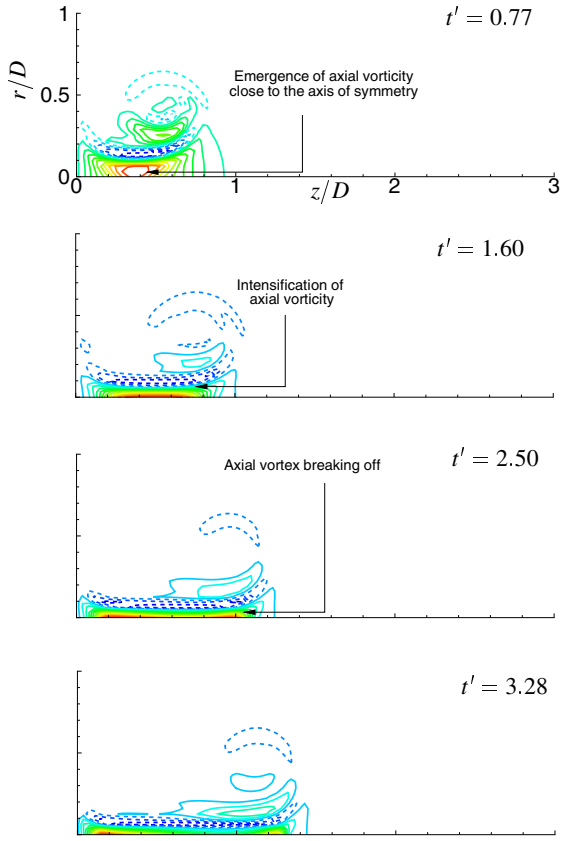

Figure 5: Evolution of contours of ω_z for Re=4020 and S=0.1.

Perhaps the most surprising observation from figure 4 is the emergence of the secondary azimuthal vorticity in front of the primary vortex ring. This could be explained by examining the

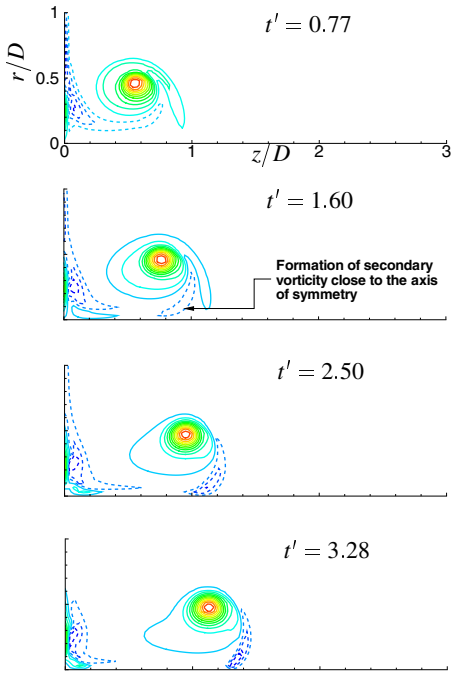

Figure 6: Evolution of contours of ω_θ for Re=4020 and S=0.1.

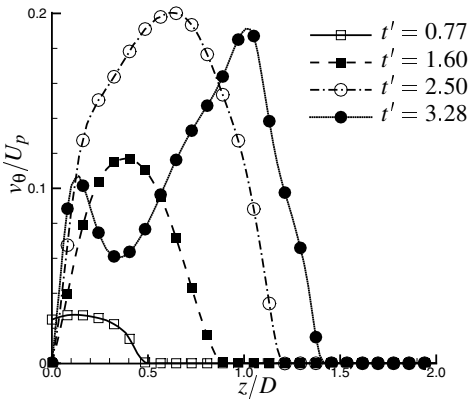

Figure 7: Evolution of v_θ for Re=4020 and S=0.1 on the $r/D = 0.1$ axis.

evolution equation for azimuthal vorticity given by

$$\frac{\partial \omega_\theta}{\partial t} = -v_r\frac{\partial \omega_\theta}{\partial r} - v_z\frac{\partial \omega_\theta}{\partial z} - \frac{v_\theta \omega_r}{r} + \omega_r\frac{\partial v_\theta}{\partial r} + \omega_z\frac{\partial v_\theta}{\partial z} + \frac{\omega_\theta v_r}{r} + \frac{1}{Re}\left[\frac{\partial}{\partial r}\left(\frac{1}{r}\frac{\partial}{\partial r}(r\omega_\theta)\right) + \frac{\partial^2 \omega_\theta}{\partial z^2}\right], \quad (6)$$

and carefully studying the evolution of ω_z, ω_θ and v_θ shown in figures 5, 6 and 7 respectively. Contours of ω_z in figure 5 shows that the imposed swirl velocity (v_θ), introduces axial vorticity into the flow field. This vorticity intensifies due to the strain field generated by the primary vortex ring. As the vortex ring is convected downstream, the axial vorticity pinches off and a

region of high (negative) axial gradient of v_θ is formed close to the axis of symmetry (see figure 7). This high axial gradient compresses azimuthal vorticity and makes $\partial\omega_\theta/\partial t$ negative (see the fifth term on the right hand side of equation (6)).

The propagation velocity of the primary vortex ring is affected by the presence of the secondary azimuthal vorticity as it induces a velocity in the opposite direction of the primary vortex ring. This is evident in figure 8 which shows contours of ω_θ at the same point in time for a simulation at $Re = 4020$ but with different values of the swirl parameter, S. It is clear that at the same values of Re, the propagation velocity of the primary vortex ring reduces with increasing values of S. Another interesting observation from figure 8 is that diameter of the primary vortex ring appear to increase for higher values of S. This is due to the presence of secondary azimuthal vorticity which induces a radial component to the propagation velocity.

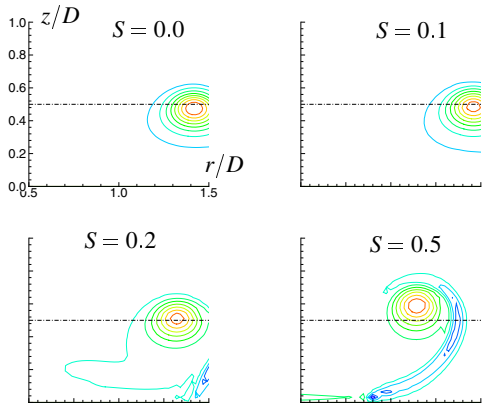

Figure 8: Contours of ω_θ for Re=4020 and different values of S. Data taken at t'=5.8.

Conclusions

Numerical simulations of the axisymmetric swirling vortex ring have been carried out at various Re and with different values of swirl parameter, S. For the reference case of a vortex ring without swirl, relatively good agreement was found between experimental data and numerical predictions. Data from the numerical simulations of the swirling vortex rings show that a secondary azimuthal vorticity is generated which is of the oppposite sign to the primary vortex ring. It was shown that this secondary azimuthal vorticity is initially generated close to the axis of symmetry and is convected away from the axis of symmetry by the primary vortex ring. The presence of the secondary azimuthal vorticity slows down the propagation velocity, U_p, of the primary vortex ring. It was also found that U_p decreases with increasing values of S.

This work is partly supported by an Expertise Program grant from the Victorian Partnership of Advanced Computing (VPAC).

References

[1] Billant P., Chomaz J. and Huerre P., Experimental study of vortex breakdown in swirling jets, *J. Fluid Mech.*, **376**, 1999, 183-219.

[2] Hicks, W.M., Researches in vortex motion-Part III. On spiral or gyrostatic vortex aggregates, *Phil Trans. R. Soc London A*, **192**, 1899, 33.

[3] Kollmann, W. and Roy, J.Y., Hybrid Navier-Stokes solver in cylindrical coordinates I:Method, *Computational Fluid Dynamics Journal*, **9**(2), 2000, 1-16.

[4] Lim TT, Vortex Rings with swirl: An experimental study. *Bulletin American Physical Society: 47th Annual meeting of the Division of Fluid Dynamics*, **39**(9), 1994, 1874.

[5] Moffatt H.K, Generalised vortex rings with and without swirl, *Fluid Dynamics Research*, **3**, 1988, 22–30.

[6] Moore, D.W. and Saffman, P.G., The motion of a vortex filament with axial flow. *Phil. Trans Roy Soc London*, **A272**, 1972, 403.

[7] Saffman, P., The velocity of viscous vortex rings, *Stud in App. Math.*, **XLIX**(4), 1970, 371.

[8] Shariff, K. and Leonard, A., Vortex Rings, *Ann Rev Fluid Mech* **235**, 1992.

[9] Turkington, B., Vortex rings with swirl: Axisymmetric solutions of the Euler equations with zero helicity. *SIAM J. Math Anal*, **20**, 1989, 57.

[10] Virk, D., Melander, M.V. and Hussain, F., Dynamics of a polarised vortex ring. *J. Fluid Mech.*, **260**, 1994, 23–55.

[11] Weigand A., Gharib M., On the evolution of laminar vortex rings. *Experiments in Fluids*, **22**, 1997, 447-457.

[12] Widnall, S.E., Bliss, D.B. and Zalay, A, Theoretical and experimental study of the stability of a vortex pair. *Aircraft wake turbulence*, editors Olsen, Golburg and Rogers, 1971, 305-308. Plenum Press, New York.